

Effect of reinforcement stiffness on the performance of reinforced soil segmental retaining walls

D.D. SAUNDERS, 1 Construction Engineering Unit, Moncton, New Brunswick, Canada
R.J. BATHURST, GeoEngineering Centre at Queen's-RMC, Geotechnical Research Group,
Royal Military College, Kingston, Ontario, Canada

ABSTRACT: The Geotechnical Research Group at the Royal Military College of Canada (RMC) is undertaking a long-term research project that includes the investigation of the performance of geosynthetic and metallic reinforced soil retaining walls during construction and under surcharge loads well in excess of working load levels. The paper examines the effect of reinforcement stiffness on wall performance by comparing selected performance results from four nominally identical segmental retaining walls that were each constructed with a different reinforcement type (i.e. two different polypropylene geogrids, a polyester geogrid and a welded wire mesh). The reinforcement materials had a narrow range of rupture strengths but a wide range of isochronous reinforcement stiffness values. The results indicate that wall performance with respect to end-of-construction connection loads, post-construction deformations under surcharging, reinforcement strain magnitudes and distributions can be related to the relative isochronous stiffness of the reinforcement materials used.

1 INTRODUCTION

The performance of several instrumented walls has indicated that the current North American design methodologies for reinforced soil segmental retaining wall (SRW) structures may be conservative (Allen 1997, Allen and Bathurst 2001). In 1998, the Geotechnical Research Group at the Royal Military College of Canada (RMC) extended a long-term research program to include reinforced soil SRW structures. The objective of the research program is to investigate the design and performance of reinforced soil retaining walls during construction, under working load levels, and subjected to loads approaching incipient wall collapse. The experimental phase of the current program involves the construction and testing of ten full-scale reinforced soil retaining walls in a controlled indoor laboratory environment. To date, six of these walls have been constructed and tested. Bathurst et al. (2001, 2002) summarise the essential details and objectives of the six test walls completed to date.

This paper summarises the experimental methodology and presents selected results from Wall 1, 2, 5 and 6 that are focused on the influence of reinforcement stiffness on the performance of walls constructed with a column of modular concrete blocks (i.e. SRW structures).

2 EXPERIMENTAL PROGRAM

2.1 Wall configurations

Each of the walls in the present test series was constructed in the RMC Retaining Wall Test Facility. The facility allows full-scale test walls to be constructed and tested under conditions approaching an idealised plane strain condition (Saunders 2001). The test walls were 3.6 m high by 3.3 m wide and in all cases the backfill soil extended approximately 6 m from the front of the facility.

Wall 1, which was the control structure, was designed using the current NCMA (1997) guidelines with the additional constraint that the reinforcement spacing not exceed a distance of twice the modular block toe-to-heel dimension (AASHTO 1998). Wall 1 was constructed with six layers of a polypropylene (PP) geogrid having low strength and stiffness properties. Each of the

subsequent walls reported here was constructed with a different reinforcement product.

Each of the test walls contained over 300 instruments to measure various aspects of wall performance. Figure 1 shows a typical instrumentation plan and test wall configuration.

2.2 Materials

The facing units used in this research program are commercially available, solid masonry blocks with a continuous shear key. During wall construction the shear key aids in maintaining a target wall batter of 8° from vertical.

The reinforcement product used in the construction of Wall 1 was a relatively weak, biaxially-drawn PP geogrid that was oriented in the machine (weak) direction. This material was chosen in order to generate large strains and deformations under uniform surcharge loading. In Wall 2, the same material was used except that every second longitudinal member was removed in order to produce a geogrid with a stiffness and strength that was 50% of that used in the control structure. Wall 5 was reinforced using a knitted PET geogrid with an index strength similar to that of the PP geogrid used in Wall 1. Wall 6 was reinforced with a commercially available 14-gauge (2-mm diameter) welded wire mesh (WWM). The mesh was manufactured with both the longitudinal and transverse members at 100-mm centres. However, every other longitudinal member was removed in order to encourage large reinforcement loads and perhaps catastrophic failure of the reinforcement with the available surcharge capacity of the RMC Retaining Wall Test Facility. This produced a mesh with a centre-to-centre spacing of 200 mm x 100 mm between longitudinal and transverse members, respectively.

Figure 2 shows the load-strain behaviour of the four different reinforcement materials used. It is worth noting that the steel reinforcement reached yield at a very low strain (approximately 0.2%) and then strain hardened until rupture. However, both the PP and PET geogrids exhibited large strains (at least 20%) prior to reaching ultimate load and rupture. Therefore, walls constructed using the extensible reinforcement products in Figure 2 may be expected to exhibit greater facing displacements, both under normal working loads and prior to wall collapse than the WWM wall in this test series.

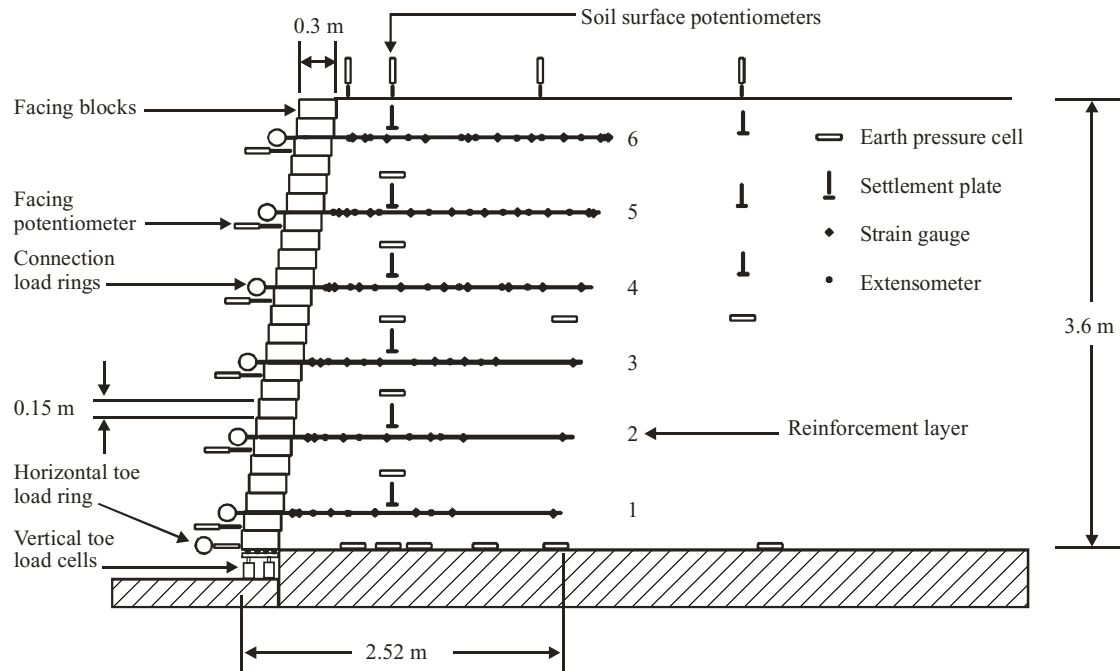


Figure 1. Cross-section and instrumentation plan for segmental walls.

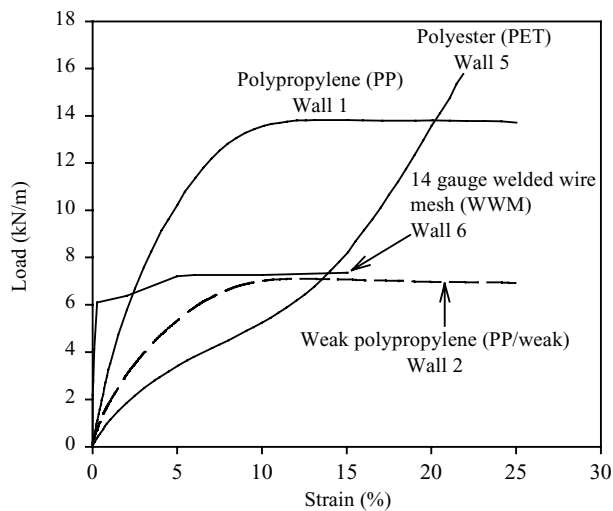


Figure 2. Reinforcement properties based on short-term tensile tests.

The reinforcement stiffness, $J(T,t)$, of a polymeric reinforcement product under a constant axial load, T , can be calculated at a prescribed elapsed time, t , from conventional in-isolation creep tests (i.e. $J(t) = T/\epsilon(t)$ where ϵ is axial strain). The stiffness values for the control PP geogrid material used in Wall 1 and the PET geogrid used in Wall 5 are illustrated in Figure 3. The figure shows that the PP geogrid has higher stiffness than the PET geogrid at short load duration (consistent with Figure 2). However, at greater elapsed times, the PP geogrid used in Wall 1 may be expected to have a reinforcement stiffness that is less than that of the PET geogrid material used in Wall 5. Finally, it should be noted that the curves for the PP geogrid used in Wall 2 can be constructed by reducing the stiffness values for the PP curves by 50%.

A uniformly graded, naturally deposited rounded beach sand (SP) having a peak plane strain friction angle, $\phi_{ps} = 44^\circ$ and a

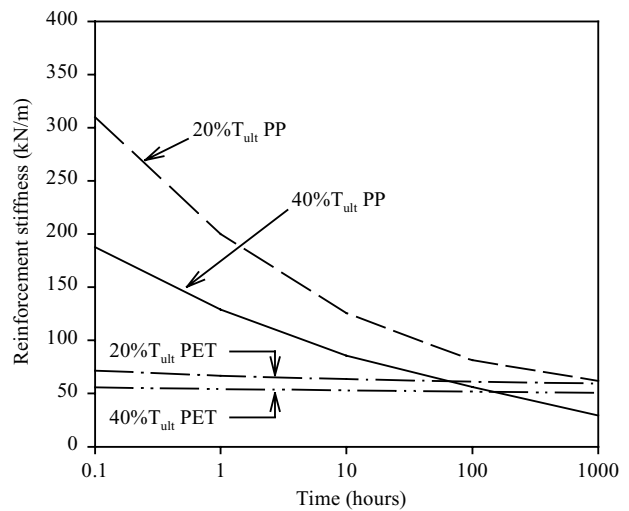


Figure 3. Reinforcement stiffness as a function of constant load level and duration of load. Note: T_{ult} = rupture strength from wide-width strip tensile testing.

constant volume friction angle, $\phi_{cv} = 35^\circ$ was used as the backfill soil in these tests. The soil was placed in 150 mm lifts and compacted using a light-weight compactor. However, in order to minimize compaction-induced stresses at the connections, the first 0.5 m behind the facing was hand tamped using a rigid steel plate.

3 MEASURED RESULTS

3.1 Facing column profiles and displacement

Bathurst et al. (2002) report that for the walls in this series, the out-of-alignment deformations from the target batter were in the range of 1 to 3% of the wall height. The out-of-alignment wall profiles were very similar for Walls 1 and 2 constructed with PP geogrids. The magnitude of lateral deformations recorded during

construction were less for the PET and WWM walls. However, the influence of reinforcement stiffness is likely masked by small variations in construction technique and compaction that are unavoidable during wall construction.

The influence of reinforcement stiffness on wall deformations can be detected more easily from measurements made during the post-construction surcharging of the walls. The maximum post-construction facing displacements during surcharging for each of the walls constructed with a rigid (modular block) facing and the same number of reinforcement layers are illustrated in Figure 4. The facing displacements have been normalized with respect to the end-of-construction profile for each wall. The duration of loading at each surcharge level was about 100 hrs for each of these structures. The facing displacements for Wall 2 were the largest recorded of all the walls. However, since Wall 2 was constructed with a reinforcement stiffness that was one-half that of the control structure, greater displacements are not unexpected.

In general, for surcharge pressures less than 60 kPa, the Wall 5 (PET) deflections were greater than those of the PP reinforced wall (Wall 1). However, beyond the 70-kPa load increment Wall 1 exhibited greater deflections. This can be explained, at least qualitatively, by the observation in Figure 3 that the stiffness of the PP geogrid material tends to decrease with time while the stiffness of the PET material is sensibly constant. The post-construction facing displacements for Wall 6 were significantly less than those of the geosynthetic reinforced walls, indicating a stiffer deflection response under surcharge loading. This is attributed to the relatively greater stiffness of the metallic reinforcement.

The greater stiffness response of Wall 5 (PET) compared to Wall 1 and 2 (PP) may also be influenced by geometry of the geogrids used and increasing load-transfer efficiency with increasing soil confinement during surcharging. During the manufacturing process multiple bundles of PET fibres are knitted together and coated, which gives the PET geogrid a rough exterior surface. Therefore, the PET may develop increasing frictional interlock with the backfill soil and less soil-geogrid interface slip with increasing confining pressure, resulting in a larger "apparent stiffness". In addition, the PET geogrid in this investigation has five additional longitudinal members per metre width than the PP geogrid (40 versus 35) and this may also have reduced the magnitude of the soil-geogrid interface slip.

3.2 Reinforcement-wall connection loads

The walls described herein were constructed with mechanical connections (i.e. the reinforcement was clamped to the modular blocks at each reinforcement elevation to simplify wall performance and to directly measure connection loads).

Figure 5 compares the measured and predicted end-of-construction connection loads for the walls. The predicted connection loads for each reinforcement layer have been calculated using the tie-back wedge approach (i.e. the contributory area multiplied by the Coulomb lateral earth pressure). The peak plane strain friction angle of the sand together with fully-mobilised soil-facing column interface friction ($\phi = \delta = 44^\circ$) were used to calculate the lateral earth pressure. In general, Coulomb lateral earth pressure theory overestimated the reinforcement connection loads. The error was greatest for the PP reinforced walls (Walls 1 and 2) and least for the WWM reinforced wall (Wall 6), which most closely approximated the predicted connection loads. The magnitude of the connection loads recorded for Wall 1 was approximately uniform with depth and was in the order of 30% of the predicted loads. The measured connection loads in Wall 5 tended to follow the trend in predicted loads (i.e. triangular) but the loads were approximately 60% of the predicted values. The over-prediction is due in part to the stiff toe restraint at the base of the wall toe that attracts a significant portion of the lateral earth force acting against the back of the facing column. The difference in magnitude of over-

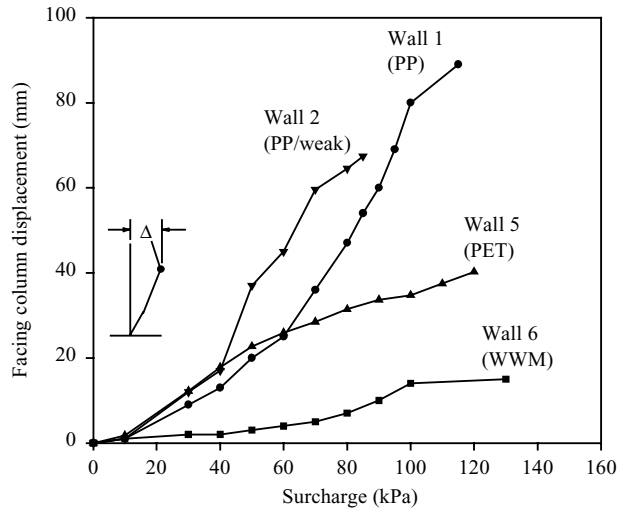


Figure 4. Overall performance of segmental walls during surcharging based on maximum post-construction facing displacement.

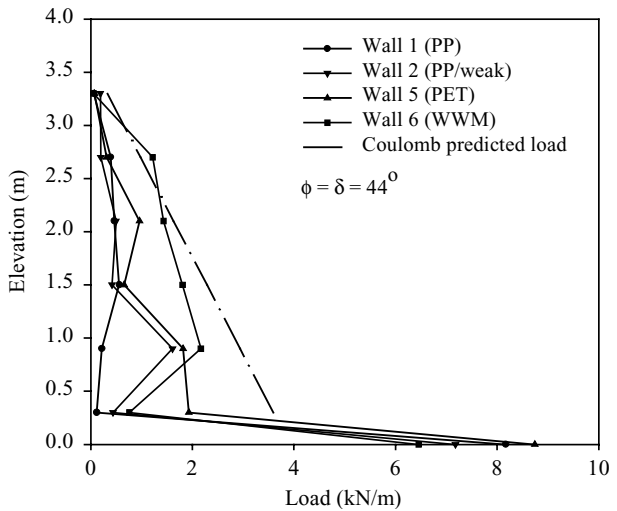


Figure 5. Connection and horizontal toe loads at the end of construction.

prediction in this set of walls can be related to relative reinforcement stiffness at the end of construction (see Figures 2 and 3). The improvement in fit between predicted and measured connection loads using the percentage values reported above is illustrated in Figure 6. However, the empirical corrections noted here apply only to the particular materials, wall height, wall geometry and boundary conditions in this test series and, working stress load levels at end of construction. Nevertheless, the comparisons emphasise that there is a potentially large underestimation of segmental retaining wall capacity against internal failure modes that should be addressed in future working-stress design methodologies.

3.3 Reinforcement strains

Figure 7 compares the strain profiles in reinforcement layer 3 of Walls 1, 2, 5, and 6 at the end of construction. The data shows that the maximum strains were at the connections but they were less than 1% for the polymeric materials and about 0.1% for the WWM wall. The greater propagation of strains along the length of the reinforcement layers for the PET and WWM walls may be related to the stiffness of the materials and soil-structure interac-

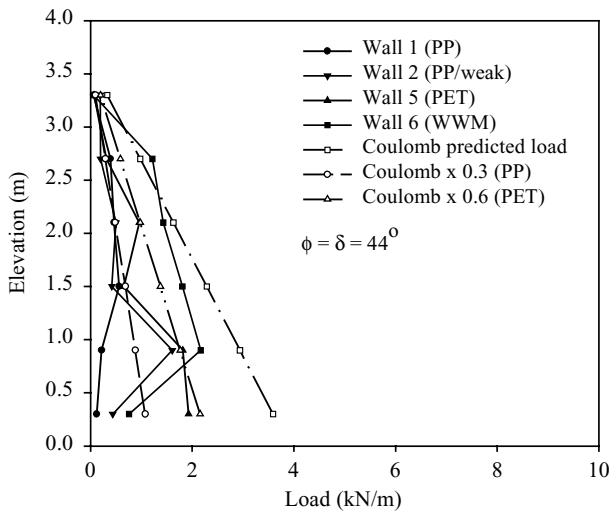


Figure 6. Empirical adjustment of reinforcement loads predicted using Coulomb earth pressure theory.

tion. Similar data is presented in Figure 8 at a common surcharge load level and reinforcement layer. The results show that there are peak strain locations in each polymeric reinforcement layer that are consistent with the notion of an internal failure surface (or surfaces) propagating through the reinforced soil zone. Based on the analysis of data obtained from backfill soil surveys taken during wall excavation, it was determined that the shape of the internal soil shear failure surface could be approximated by a log spiral curve. Peak strain locations for the WWM reinforced wall were difficult to determine which is consistent with the absence of a visually-apparent internal failure mechanism during wall excavation.

4 CONCLUSIONS

The data from the walls described here illustrate that the isochronous stiffness properties of the reinforcement materials can explain the relative performance difference between nominally identical SRW structures with respect to wall deformations, connection loads and magnitude of reinforcement strains.

ACKNOWLEDGEMENTS

The writers would like to acknowledge the financial support of the following US State Departments of Transportation: Washington, Alaska, Arizona, California, Colorado, Idaho, Minnesota, New York, North Dakota, Oregon, Utah, and Wyoming. The writers are also grateful for the financial support of the National Concrete Masonry Association, the Reinforced Earth Company, Natural Sciences and Engineering Research Council of Canada, and grants from the Department of National Defence (DND Canada). The authors would like to acknowledge the contribution of materials by Risi Stone Systems, Terrafix Inc., Strata Systems Inc. and Modular Gabion Systems. The authors also wish to thank David Walters for providing many helpful suggestions during the preparation of the paper.

REFERENCES

AASHTO. 1998. *Interims: Standard Specifications for Highway Bridges*, American Association of State Highway and Transportation Officials, Washington, D.C., USA.

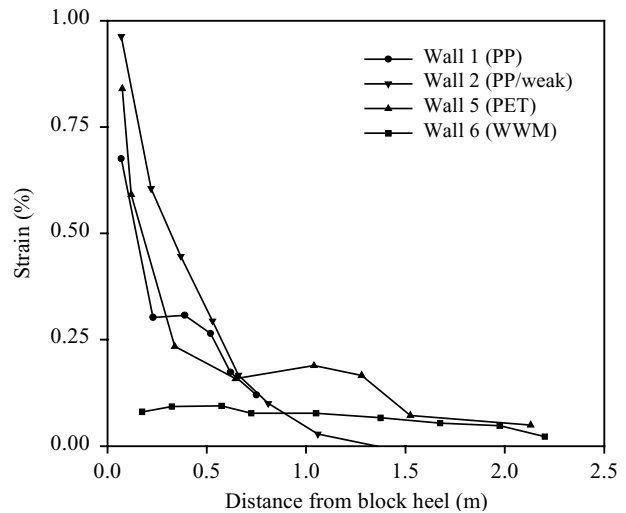


Figure 7. Strain distribution in layer 3 at the end of construction.

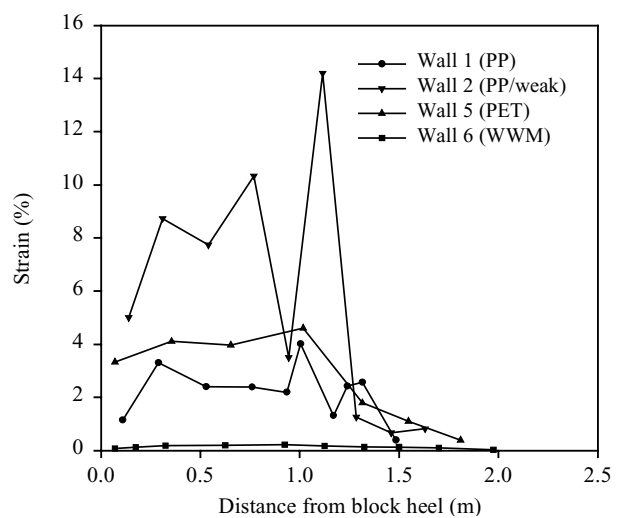


Figure 8. Strain distribution in layer 5 at the end of 80 kPa surcharge load level.

- Allen, T. M. & Bathurst, R. J. 2001, *Prediction of Soil Reinforcement Loads in Mechanically Stabilized Earth (MSE) Walls*, Washington State Department of Transportation, Report WA-RD 522.1, 353 pp.
- Allen, T.M. 1997. Current Code Versus Reality, *Mechanically Stabilized Backfill*, Edited by J.T.H. Wu, Proceedings of the International Symposium on Mechanically Stabilized Backfill (MSB), Denver, Colorado, USA, February 1997, pp. 335-339.
- Bathurst, R.J., Walters, D., Hatami, K. & Allen, T.M. 2001. Full scale performance testing and numerical modelling of reinforced soil retaining walls (Invited Keynote paper). In H. Ochiai, J. Otani, N. Yasufuku & K. Omine (eds), *Landmarks in Earth Reinforcement, IS Kyushu 2001; Proc. Inter. Symp., 14-16 November 2001*. (preprint).
- Bathurst R.J., Walters, D.L., Hatami, K., Saunders, D.D., Vlachopoulos, N.P., Burgess, G.P. & Allen, T.M. 2002. Performance Testing and Numerical Modelling of Reinforced Soil Retaining Walls, *7th International Conference on Geosynthetics*, Nice, France, September 2002.
- NCMA. 1997. *Design Manual for Segmental Retaining Walls*, Second Edition, Second Printing, National Concrete Masonry Association, Herndon, Virginia, USA, 289 p.
- Saunders, D.D. 2001. The Performance of a Full-Scale Polyester Geogrid Reinforced Segmental Retaining Wall, *Geosynthetics Conference 2001*, Portland, Oregon, USA, February 2001, pp. 579-588.